Communication

Metallic Mesoporous Nanocomposites for Electrocatalysis

Yi Ding, Mingwei Chen, and Jonah Erlebacher

J. Am. Chem. Soc., **2004**, 126 (22), 6876-6877• DOI: 10.1021/ja0320119 • Publication Date (Web): 14 May 2004

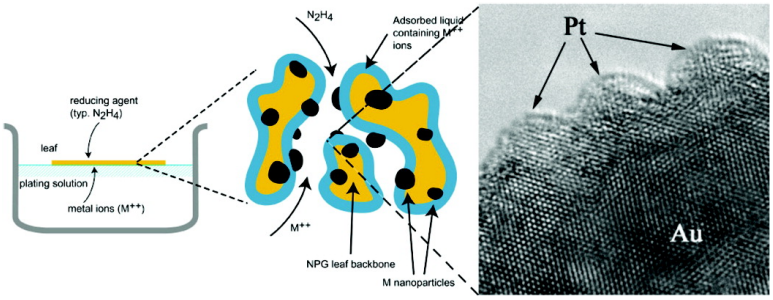

More About This Article

Additional resources and features associated with this article are available within the HTML version:

- Supporting Information
- Links to the 14 articles that cite this article, as of the time of this article download
- Access to high resolution figures
- Links to articles and content related to this article
- Copyright permission to reproduce figures and/or text from this article

View the Full Text HTML

J|A|C|S
COMMUNICATIONS

Published on Web 05/14/2004

Metallic Mesoporous Nanocomposites for Electrocatalysis

Yi Ding,[†] Mingwei Chen,[‡,§] and Jonah Erlebacher*[,†]

Department of Materials Science and Engineering, Johns Hopkins University, Baltimore, Maryland 21218, Department of Mechanical Engineering, Johns Hopkins University, Baltimore, Maryland 21218, and Institute for Materials Research, Tohoku University, Sendai, Japan

Received December 31, 2003; E-mail: jonah.erlebacher@jhu.edu

A significant effort has been made to develop highly porous catalytic electrodes for many important technologies involved in energy conversion, e.g., fuel cells.[1] Commonly, a nanoparticle-based materials design strategy has been employed in which catalytic nanoparticles are physisorbed onto a conductive and corrosion-resistant support substrate, such as carbon black.[2] However, in such designs, nanoparticles are usually only weakly adsorbed to carbon, and there is a tendency for them to agglomerate over time under operating conditions, reducing their active surface area and limiting device lifetime.[3,4] Here we describe a new kind of electrocatalytically active metallic mesoporous nanocomposite made by creating an atomically thin layer of platinum over a nanoporous gold core. In comparison to nanoparticle catalysts supported on carbon black, these membranes simultaneously provide superior catalyst/substrate binding as well as provide a high volume dispersion of catalyst uniformly distributed through a very thin porous electrode with high in-plane conductivity.

The ideal catalytically functionalized electrode will consist of an inert, conductive, porous substrate in the form of a membrane on which is uniformly coated an atomically thin layer of a catalytic material such as platinum.[1] In this way, precious metal catalyst atoms are most likely to reside on a surface, and not be buried and thus inactive;[5,6] this optimizes their utility from a cost perspective. A good candidate substrate is a membrane of nanoporous gold (NPG) leaf made by dealloying 12-carat, 100 nm thick white gold leaf.[7] NPG leaf contains a very small amount of gold (per area of the membrane, the gold content, or loading, is only 0.12 mg cm^{-2}) but contains a large specific surface area of order 10 m^2 g^{-1}, has high in-plane conductivity, and is inert. It is easy to envision that other, nonprecious mesoporous metal membranes may be fabricated by similar methods.

Platinum-coated NPG membranes are made by placing the porous membrane at the interface between a solution containing metal ions in suspension and a vapor of a reducing agent. By separating the reactants in this way, the plating reaction is confined to occur uniformly on surfaces within the pores and not create a skin on one side of the membrane as would occur using standard plating methods.[7] Deposition of platinum by this method creates the desired microstructure of an atomically thin catalyst skin uniformly coating a conductive substrate. The deposition is self-limiting and saturates at loadings of 0.06 mg cm^{-2} as determined by energy-dispersive X-ray spectroscopy (EDS) measurements. Typical deposition times are on the order of minutes and can be halted easily by removing the reducing atmosphere. This plating method thus allows exquisite control over platinum loading of the membrane to within 0.01 mg cm^{-2} (over the 100 nm thickness of the membrane) using only simple benchtop processing at room temperature.

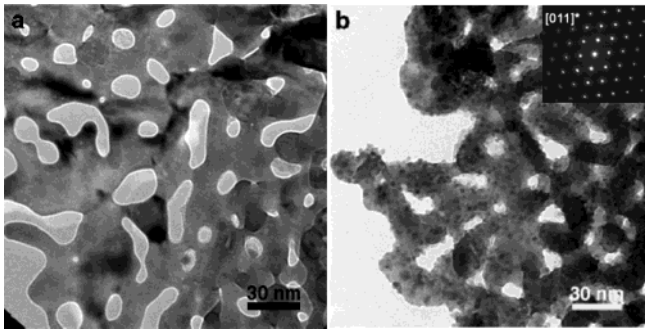

Figure 1. TEM images of NPG leaf before and after Pt plating. (a) NPG leaf; (b) Pt-NPG sample after plating for 24 min. The inset diffraction pattern in (b) shows the single-crystal nature of the Pt-NPG composites, indicating a coherent crystallographic relationship between plated Pt nanoparticles and the gold substrate (the diffraction pattern was measured off a sample plated for 192 min). The plating process is similar to that reported in ref 7, and for all work reported herein, the plating solution contains 2 mM $Na_2Pt(OH)_6$ salt with a pH value at 9.9, using hydrazine gas as the reducing agent. White gold leaf was purchased from Sepp Leaf Products Inc. (New York).

Figure 1 shows transmission electron microscope (TEM) images of porous gold leaf (a) before and (b) after platinum plating and illustrates the structural length scales of these materials as well as the highly uniform volume dispersion of catalyst. The three-dimensional bi-continuous porous structure can be seen in NPG leaf with a pore size around 15 nm (Figure 1a). This pore size is significantly smaller than the lateral grain size of the membrane, which is on the order of a few microns. That means the micrograph shown in Figure 1a was recorded from one porous single-crystal grain. The single-crystal nature of the NPG substrate can be clearly seen from the high-resolution electron microscope (HREM) image shown in Figure 2a, where lattice fringes extend continuously from one ligament to the other by viewing the image at grazing incidence along ⟨200⟩ directions. A slight lattice distortion is frequently seen on the porous surface as indicated by the inserted fast Fourier transform (FFT) pattern and is possibly due to surface stress or the presence of a reconstruction.[8]

Upon plating, highly dispersed Pt islands uniformly cover the porous structure, as shown in Figure 1b. These islands have a very narrow size distribution between 2 and 4 nm (Figure 1b). Interestingly, the single-crystal character of the support was retained in Pt plated NPG leaf. Even with the relatively high platinum loading (0.05 mg cm^{-2}) in the 192-min sample, electron diffraction still yields single-crystal diffraction patterns with only slight diffuse streaks along ⟨110⟩ directions from this composite nanostructure (see the inset of Figure 1b). This observation indicates a coherent crystallographic relationship between deposited Pt and the NPG substrate, evidence for an epitaxial growth mode of Pt on the NPG substrate rather than adsorption of individual Pt nanoparticles. HREM observations with atomic resolution confirm this coherent

[†] Department of Materials Science and Engineering, Johns Hopkins University.
[‡] Department of Mechanical Engineering, Johns Hopkins University.
[§] Tohoku University.

10.1021/ja0320119 CCC: $27.50

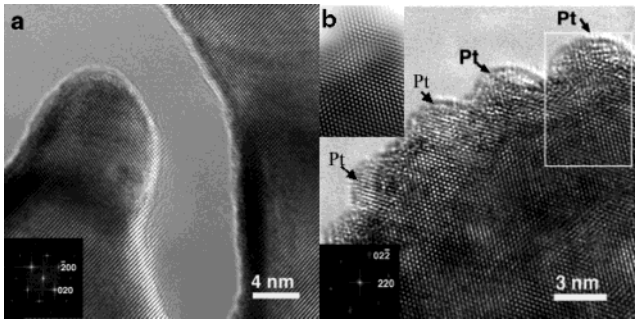

Figure 2. HREM images of (a) NPG leaf and (b) Pt-NPG, 24 min plating. The coherent crystal relationship between Pt nanoparticles and Au matrix can be determined as $\langle 110\rangle_{Au}//\langle 110\rangle_{Pt}$ and $\{111\}_{Au}//\{111\}_{Pt}$. The slight lattice distortions at the interface between Pt particle and Au matrix as highlighted in the inserted Fourier filtered image suggests a strained epitaxial growth mode.

relationship. As shown in Figure 2b, Pt islands are hemispherical, and two sets of lattice fringes ⟨110⟩ extend continuously from gold to platinum. In addition, a lattice distortion is found at the interface between Pt and Au and is highlighted in the inset Fourier-filtered image. Plated islands are generally 3 nm in diameter with a height of just a few atomic layers. This Pt-NPG nanocomposite is very stable and no Pt aggregation or coarsening of the mesoporous support was found after sitting at ambient temperature for over 2 months, nor after annealing at 300 °C for periods of order 1 h.

If the growth reaction were limited by transport of either Pt ions or reducing agent into the pores, it may be thought that there would be a gradient in the catalyst island size through the thickness of the membrane, which we do not see. This observation combined with the TEM results suggests the following hypothesis regarding this unusual growth mode: when an isolated Pt island nucleates on a region of NPG substrate it begins by growing coherently to the substrate because both materials possess a face-centered cubic (fcc) crystal structure. There will be no mixing across the interface because gold and platinum are practically immiscible at room temperature.[9] However, due to a 4% lattice mismatch between gold and platinum, as the Pt island grows it will become highly strained in order to maintain coherency between itself and the substrate (the high curvature of the NPG substrate will only exacerbate this effect), and this may create a barrier to further platinum incorporation from solution with the effect of slowing growth. At a particular critical size, it will be energetically favorable to nucleate new islands nearby rather than continue growth of or nucleate defects within the first one. We believe this crystallographic and thermodynamic control from the growth system itself over the size and structure of heterogeneously nucleated nanoparticles is unique to other wet-chemistry based nanoparticle fabrication methods[10] where surfactants are always necessary to prevent the aggregation and coarsening of active nanoparticles and may find applications in other fields.

To prove the general utility of our mesoporous nanocomposite electrodes, a functional, homemade proton exchange membrane fuel cell employing Pt-NPG electrodes was fabricated, and it shows good device performance. To make the cell, we dried two pieces of Pt-NPG leaf (0.04 mg cm^{-2} Pt loading) onto a sheet of Nafion 112

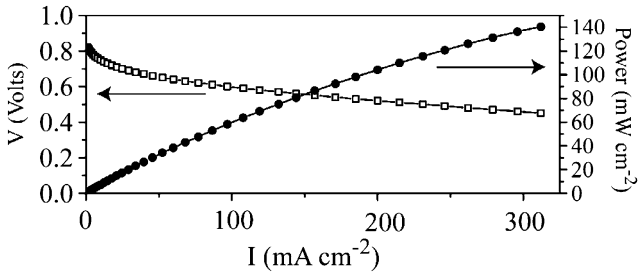

Figure 3. Cell voltage and power density versus current density for a Pt-NPG membrane fuel cell. The cell electrodes have a Pt loading of 0.04 mg cm^{-2} on each side.

polymer electrolyte, one on each side. Upon air-drying, the sandwich structure was heated at 140 °C for 2 min to form a completed membrane electrode assembly (MEA). This heating step serves to pull ionomer into the pores of the Pt-NPG leaf, improving adhesion between the Nafion and the electrode and also creating pathways for proton conduction from within the electrode to the ionomer. In this way the region of three-phase contact of the fuel cell containing active catalyst is confined to within a 100 nm thick layer. The MEA was sandwiched between two pieces of Toray carbon paper, and this structure was in turn sandwiched between two graphite current collection plates on which gas flow channels had been machined into an area of 1 cm^2. A typical polarization curve for the cell running with H_2 and O_2 bubbled through water at room temperature and atmospheric pressure is shown in Figure 3. Although our cells have not been tested under rigorous operating conditions, typical $I-V$ curves are characterized by an open circuit voltage near 0.9 V, a short circuit current density near 0.5 A cm^{-2}, and a maximum power density greater than 0.14 W cm^{-2}. On a per gram basis, our cell generated 1.75 kW g^{-1} Pt, which compares favorably to the performance of good commercially available MEAs, which typically generate a peak power near 1.0 W cm^{-2} with loading of 0.5 mg of Pt cm^{-2} on each electrode (a specific power of order 1.0 kW g^{-1}).[1]

Acknowledgment. This work is supported by the NSF under Grant 0092756. Technical assistance in fuel cell fabrication and assessment by D. Gervasio (ASU) and B. Pivovar (LANL) is gratefully acknowledged.

References

(1) Steele, B. C. H.; Heinzel, A. *Nature* **2001**, *414*, 345.
(2) Larminie, J.; Dicks, A. *Fuel Cell Systems Explained*, 2nd ed.; John Wiley & Sons: Ltd. Hoboken, NJ, 2003.
(3) Campbell, C. T.; Parker, S. C.; Starr, D. E. *Science* **2002**, *298*, 811.
(4) Blom, D. A.; Dunlap, J. R.; Nolan, T. A.; Allard, L. F. *J. Electrochem. Soc.* **2003**, *150*, A414.
(5) Anderson, M. L.; Stroud, R. M.; Rolison, D. R. *Nano Lett.* **2002**, *2*, 235.
(6) Wilson, M. S.; Garzon, F. H.; Sickafus, K. E.; Gottesfled, S. *J. Electrochem. Soc.* **1993**, *140*, 2872.
(7) Ding, Y.; Erlebacher, J. *J. Am. Chem. Soc.* **2003**, *125*, 7772.
(8) Newman, R. C.; Sieradzki, K. *Science* **1994**, *263*, 1708.
(9) Massalski, T. B. Ed.; *Binary Alloy Phase Diagrams*; Materials Park, OH; ASM, 1990.
(10) Jana, N. R.; Peng, X. *J. Am. Chem. Soc.* **2003**, *125*, 14280.

JA0320119